

## Research Article

# Multistability and Self-Similarity in the Parameter-Space of a Vibro-Impact System

Silvio L. T. de Souza,<sup>1</sup> Iberê L. Caldas,<sup>2</sup> and Ricardo L. Viana<sup>3</sup>

<sup>1</sup> Universidade Federal de São João del-Rei, Campus Alto Paraopeba, Km 7 Rodovia MG 443, 36420-000 Ouro Branco, Minas Gerais, Brazil

<sup>2</sup> Instituto de Física, Universidade de São Paulo, 05315-970 São Paulo, Brazil

<sup>3</sup> Departamento de Física, Universidade Federal do Paraná, 81531-990 Curitiba, Paraná, Brazil

Correspondence should be addressed to Ricardo L. Viana, viana@fisica.ufpr.br

Received 22 April 2009; Accepted 23 June 2009

Recommended by Edson Denis Leonel

The dynamics of a dissipative vibro-impact system called impact-pair is investigated. This system is similar to Fermi-Ulam accelerator model and consists of an oscillating one-dimensional box containing a point mass moving freely between successive inelastic collisions with the rigid walls of the box. In our numerical simulations, we observed multistable regimes, for which the corresponding basins of attraction present a quite complicated structure with smooth boundary. In addition, we characterize the system in a two-dimensional parameter space by using the largest Lyapunov exponents, identifying self-similar periodic sets.

Copyright © 2009 Silvio L. T. de Souza et al. This is an open access article distributed under the Creative Commons Attribution License, which permits unrestricted use, distribution, and reproduction in any medium, provided the original work is properly cited.

## 1. Introduction

In order to study cosmic ray accelerated to high energy, Enrico Fermi proposed an accelerator model as a dynamical system [1], consisting of a classical particle interacting with a time dependent magnetic field. The original model was later modified and studied under different approaches. For example, the dynamics of the well-known Fermi-Ulam model has been investigated [2]. This model consists of a point mass moving between a rigid fixed wall and an oscillatory wall. In the recent years, the Fermi-Ulam model has attracted a significant attention to understand the dynamics of systems with limited energy gain, for certain parameters and initial conditions, in contrast with the Fermi acceleration [3–6].

In the engineering context, mathematical models describing mechanical impacts similar to those considered in the Fermi-Ulam model have been intensively studied, like gearbox model [7–10] and impact damper [11, 12]. These systems, called vibro-impact or impact oscillator, appear in a wide range of practical problems, such as percussive drilling

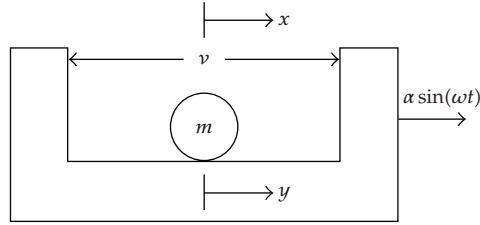


Figure 1: Schematic view of an impact-pair system.

tools [13], print hammers [14], and vibro-impact moling systems [15], just to mention a few. For these systems a better understanding of their dynamics may help to reduce the negative effects of impacts and ultimately to improve practical designs. Although the results obtained for the impact oscillator have different interpretations, the mathematical analyses are similar to those used to investigate the Fermi-Ulam model.

In this paper, we consider a prototypical vibro-impact system, known as impact-pair. This system is comprised of a ball moving between two oscillatory walls. Numerical studies have shown a rich dynamical behavior with several nonlinear phenomena observed, such as bifurcations, chaotic regimes [16, 17], crises [18], and basin hoppings [19]. In addition, control of chaotic dynamics can be applied to stabilize unstable periodic orbits embedded in the chaotic attractor [20]. We aim here to explore some dynamical properties with emphasis on characterization of basins of attraction with complicated smooth boundaries and identification of self-similar periodic sets called shrimps [21].

This paper is organized as follows. In Section 2 we present the model and the equations of motion for the impact-pair system. In Section 3, we investigate coexistence of different regimes and their basins of attraction. In Section 4, we characterize the impact-pair system in the two-parameter space. The last section contains our conclusions.

## 2. Mathematical Description

In this section we present the basic equations of the impact-pair system [16, 17] shown schematically in Figure 1. In addition, following the mathematical description of [19], we describe how to obtain an impact map, also called transcendental map. The map is useful to calculate the Lyapunov exponents [18].

The impact-pair system is composed of a point mass  $m$ , whose displacement is denoted by  $x$ , and a one-dimensional box with a gap of length  $\nu$ . The mass  $m$  is free to move inside the gap and the motion of the box is described by a periodic function,  $\alpha \sin(\omega t)$ .

In an absolute coordinate systems, equation of motion of the point mass  $m$  is given by

$$\ddot{x} = 0. \quad (2.1)$$

On denoting the relative displacement of the mass  $m$  by  $y$ , we have

$$x = y + \alpha \sin(\omega t), \quad (2.2)$$

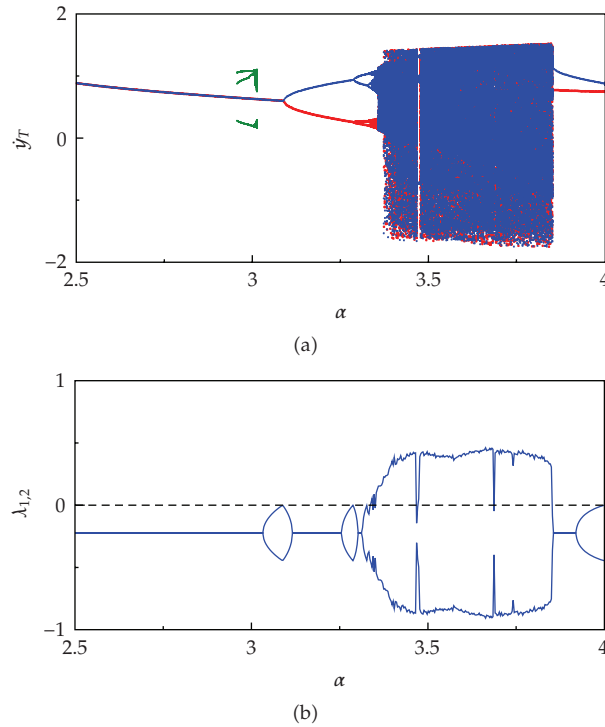


**Figure 2:** (a) Bifurcation diagram showing coexisting attractors. Velocity  $\dot{y}_T$ , for a stroboscopic map, as a function of the amplitude excitation,  $\alpha$ , for  $r = 0.8$ . (b) The Lyapunov exponents,  $\lambda_{1,2}$ , for the attractors plotted in blue.

such that, on substituting (2.2) into (2.1), the equation of motion in the relative coordinate system is

$$\ddot{y} = \alpha\omega^2 \sin(\omega t), \quad \left(-\frac{\nu}{2} < y < \frac{\nu}{2}\right). \quad (2.3)$$

Integrating (2.3) and for the initial conditions  $y(t_0) = y_0$  and  $\dot{y}(t_0) = \dot{y}_0$ , the displacement  $y$  and the velocity  $\dot{y}$ , between impacts, are

$$\begin{aligned} y(t) &= y_0 + \alpha \sin(\omega t_0) - \alpha \sin(\omega t) + [\dot{y}_0 + \alpha\omega \cos(\omega t_0)](t - t_0), \\ \dot{y}(t) &= \dot{y}_0 + \alpha\omega \cos(\omega t_0) - \alpha\omega \cos(\omega t). \end{aligned} \quad (2.4)$$

An impact occurs wherever  $y = \nu/2$  or  $-\nu/2$ . After each impact, we apply into (2.4) the new set of initial conditions (Newton's law of impact)

$$t_0 = t, \quad y_0 = y, \quad \dot{y}_0 = -r\dot{y}, \quad (2.5)$$

where  $r$  is a constant restitution coefficient.

Therefore, the dynamics of the impact-pair system is obtained from (2.4) and (2.5). In this case, the system depends on control parameters  $\nu$ ,  $r$ ,  $\alpha$ , and  $\omega$ .

Since there is an analytical solution for the motion between impacts, we can obtain an impact map. First, we define the discrete variables  $y_n$ ,  $\dot{y}_n$ ,  $t_n$  as the displacement, the velocity, and the time (modulo  $2\pi$ ) collected just the  $n$ th impact. Substituting the Newton law of impact into (2.4), we have a two-dimensional map that is given by

$$\begin{aligned} y_{n+1} &= y_n + \alpha \sin(\omega t_n) - \alpha \sin(\omega t_{n+1}) + [-r\dot{y}_n + \alpha\omega \cos(\omega t_n)](t_{n+1} - t_n), \\ \dot{y}_{n+1} &= -r\dot{y}_n + \alpha\omega \cos(\omega t_n) - \alpha\omega \cos(\omega t_{n+1}), \end{aligned} \quad (2.6)$$

where  $y_n = v/2$  or  $-v/2$ .

As mentioned before, this map, obtained by considering the analytical solutions and the sequence of impact times, is only used to evaluate the Lyapunov exponents [18]. The system dynamics is directly analyzed from the analytical solutions of (2.4) and (2.5). The Lyapunov exponents are computed through

$$\lambda_i = \lim_{n \rightarrow \infty} \frac{1}{n} \ln |\Lambda_i(n)| \quad (i = 1, 2), \quad (2.7)$$

where  $\Lambda_i(n)$  are the eigenvalues of the matrix  $A = J_1 \cdot J_2 \cdot \dots \cdot J_n$  with  $J_n$  being the Jacobian matrix of the map (2.6), computed at time  $n$ . For systems without analytical solutions between the impacts, the Lyapunov exponents can be calculated by using the method proposed by Jin et al. [22].

### 3. Multistability with Complex Basins of Attraction

The dynamics was investigated using bifurcation diagrams, phase portraits, Lyapunov exponents, basins of attraction, uncertainty exponent, and parameter space diagrams. We fix the control parameters at  $v = 2.0$  (length of the gap),  $\omega = 1.0$  (excitation frequency) and vary the parameters  $r$  (restitution coefficient) and  $\alpha$  (excitation amplitude).

In order to obtain a representative example of the kind of dynamics generated by the impact-pair system, we use a bifurcation diagram for the velocity,  $\dot{y}_T$ , versus the amplitude excitation,  $\alpha$ . The dynamical variable  $\dot{y}_T$  is obtained from a stroboscopic map (Time- $2\pi$ ). To characterize the nature of the behavior observed, we calculate the Lyapunov exponents. If the largest Lyapunov exponent is positive the attractor is chaotic, if not the attractor is periodic.

In Figure 2(a), we present a bifurcation diagram showing multiple coexisting attractors plotted in different colors. For example, we can note two period-1 orbits at  $\alpha = 3.2$ . In this case, these attractors are symmetric and appear due to the pitchfork bifurcation for  $\alpha \approx 3.0878$ . For  $\alpha \approx 3$ , the diagram shows two coexisting attractors depicted in green and blue. The Lyapunov exponents for attractors plotted in blue are shown in Figure 2(b).

In Figures 3(a) and 3(b), we show the phase portraits of the two symmetrical coexisting periodic attractors for  $\alpha = 3.2$ . For the same set of parameters, we identify two more other possible solutions, namely, two equilibrium points shown in Figures 3(c) and 3(d).

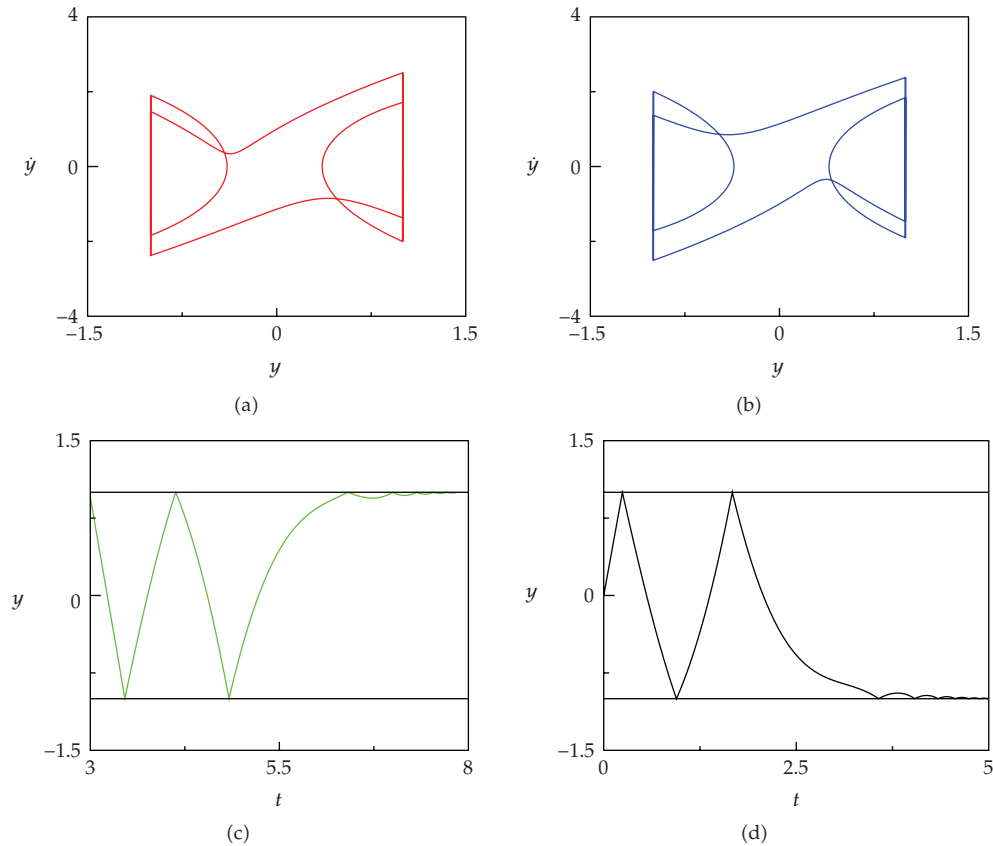


**Figure 3:** Phase portrait of velocity versus displacement of two coexisting periodic attractors (a) and (b). Time histories of two equilibrium points (c) and (d). For the control parameters  $\alpha = 3.2$  and  $r = 0.8$ .

The corresponding basins of attraction of the four possible solutions are depicted in Figure 4(a). This figure is constructed using a grid of equally spaced  $1000 \times 1000$  cells as set of initial conditions for velocity *versus* time (*modulo*  $2\pi$ ) with initial position fixed at  $y_0 = 0$ . The basins of the periodic attractors are plotted in blue and red, and the equilibrium points in white and green.

As can be seen, the structure of the basins is quite complex and the basin boundary between periodic attractors is convoluted and apparently fractal (Figures 4(b) and 4(c)). However, in contrast to fractal basin boundaries, we cannot observe an infinitely fine scaled structure with magnifications of the boundary region, as shown in Figure 4(d). Therefore, the basin boundary here is composed of smooth curve with dimension one. In this case, the complexity of basins structure is generated by band accumulations [23–25]. Moreover, the observed smooth basin boundary was also observed for other parameter regions with coexisting periodic or chaotic attractors.

As a consequence of the complex basins of attraction observed, uncertainty in initial conditions leads to uncertainty in the final state. To evaluate the final state sensitivity we can calculate the uncertainty exponent,  $\beta$ , which was proposed by Grebogi and his collaborators [26] and has been used to characterize fractal basin boundaries [10, 12].

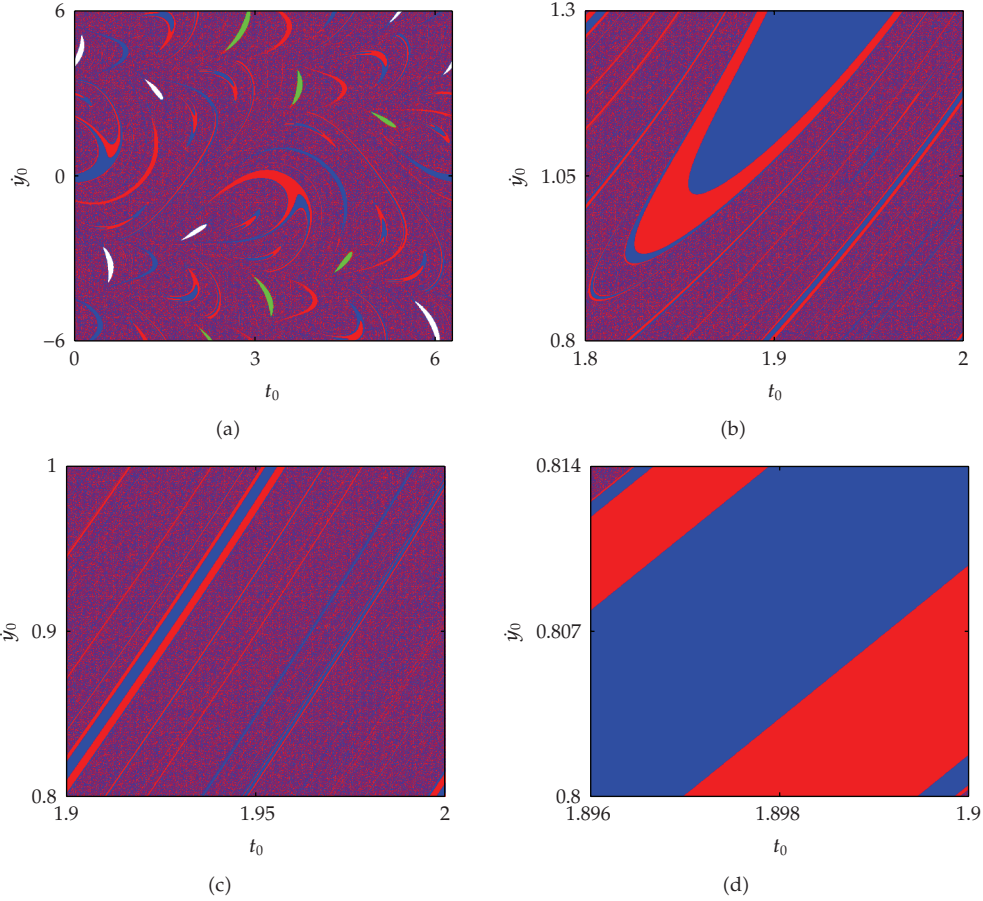


**Figure 4:** Basins of attraction and successive magnifications for the parameters  $\alpha = 3.2$  and  $r = 0.8$ , varying initial conditions  $\dot{y}_0$  and  $t_0$  with  $y_0 = 0$ . Basins in red and blue for the two coexisting attractors were shown in Figures 3(a) and 3(b) basins, in green and white for the two equilibrium points were shown in Figures 3(c) and 3(d).

To obtain the uncertainty exponent, we choose randomly a large number of set initial conditions  $A : (\tau_0, \dot{y}_0)$  for  $y_0$  constant. We keep  $\dot{y}_0$  constant and vary the other coordinate by a small amount  $\epsilon$ . We also choose the slightly displaced initial conditions  $B : (\tau_0 + \epsilon, \dot{y}_0)$  and  $C : (\tau_0 - \epsilon, \dot{y}_0)$ . If the trajectory starting from initial condition  $A$  goes to one of the basins, and either one (or both) of the displaced initial conditions,  $B$  or  $C$ , go to the other basin, we call  $A$  as an  $\epsilon$ -uncertain initial condition. By considering a large number of such points, we can estimate the fraction of  $\epsilon$ -uncertain points,  $f(\epsilon)$ . This number scales with the uncertain radius as a power-law  $f(\epsilon) \sim \epsilon^\beta$ , where  $\beta$  is called uncertainty exponent [24, 26].

For the basins of attraction shown in Figure 4(c), we obtain the uncertainty exponent  $\beta = 0.490 \pm 0.001$ , as indicated in Figure 5. In this case, if we want to gain a factor 2 in the ability to predict the final state of the system, it is necessary to increase the accuracy of initial condition by a factor approximately 4 ( $2^{1/0.49} \approx 4$ ). In general a noninteger uncertainty exponent is a consequence of a fractal basin boundary. However, in this case the considered boundary is smooth with a dimension  $d_B = 1$ ; but even so the uncertainty to predict the final state remains.

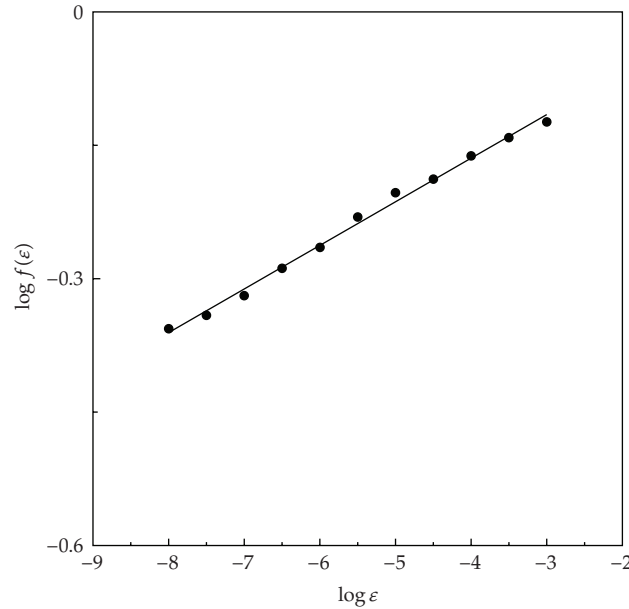


**Figure 5:** Uncertain fraction versus uncertainty radius  $\epsilon$  for basins of attraction showed in Figure 4(c) for  $\alpha = 3.2$  and  $r = 0.8$ . The solid curve is a linear regression fit with slope  $\beta = 0.490 \pm 0.001$ .

#### 4. Self-Similar Periodic Sets in Parameter Space

In order to obtain a further insight into the influence of the restitution coefficient  $r$  and amplitude excitation  $\alpha$  on the dynamics of the impact-pair system, we construct parameter space diagrams, depicted in Figures 6(a) to 6(d). To obtain these diagrams, we use a grid of  $1000 \times 1000$  cells with the initial conditions fixed at  $(y_0, \dot{y}_0, \tau_0) = (0, 1, 0)$ . For each point the largest Lyapunov exponent is calculated and plotted with the appropriately allocated color. Chaotic attractors ( $\lambda_1 > 0$ ) are plotted in blue and periodic attractors ( $\lambda_1 < 0$ ) according to a color scale ranging from minimum value in red and maximum in green. Zero Lyapunov exponents (bifurcation points) are plotted in blue.

To clarify how the parameter space diagram was constructed, we fix the restitution coefficient at  $r = 0.683$  for Figure 6(c) and vary the amplitude excitation  $\alpha$  determining bifurcation diagram and the corresponding largest Lyapunov exponents in Figures 7(a) and 7(b), respectively. Comparing the Lyapunov exponents with parameter space diagram (Figure 6(c)), we can note that red lines correspond with the local minimum of exponents and blue lines embedded in green region (periodic region) correspond with bifurcation points.

On examining the parameter space diagram (Figure 6(b)), we note a main periodic structure existing embedded in chaotic region. Around this structure a vast quantity of self-similar periodic sets is found. For instance, we can see in Figure 6(c) a very regular network of self-similar structures for a magnification of small box of Figure 6(b). These self-similar structures have been observed before [27–31] and have been referred to as shrimps [32–34]. In our work, the shrimps organize themselves along a very specific direction in parameter space with a series of accumulations and fractality can be observed with successive magnifications of the parameter space, as shown in Figure 6(d) for a magnification of a shrimp of Figure 6(c).

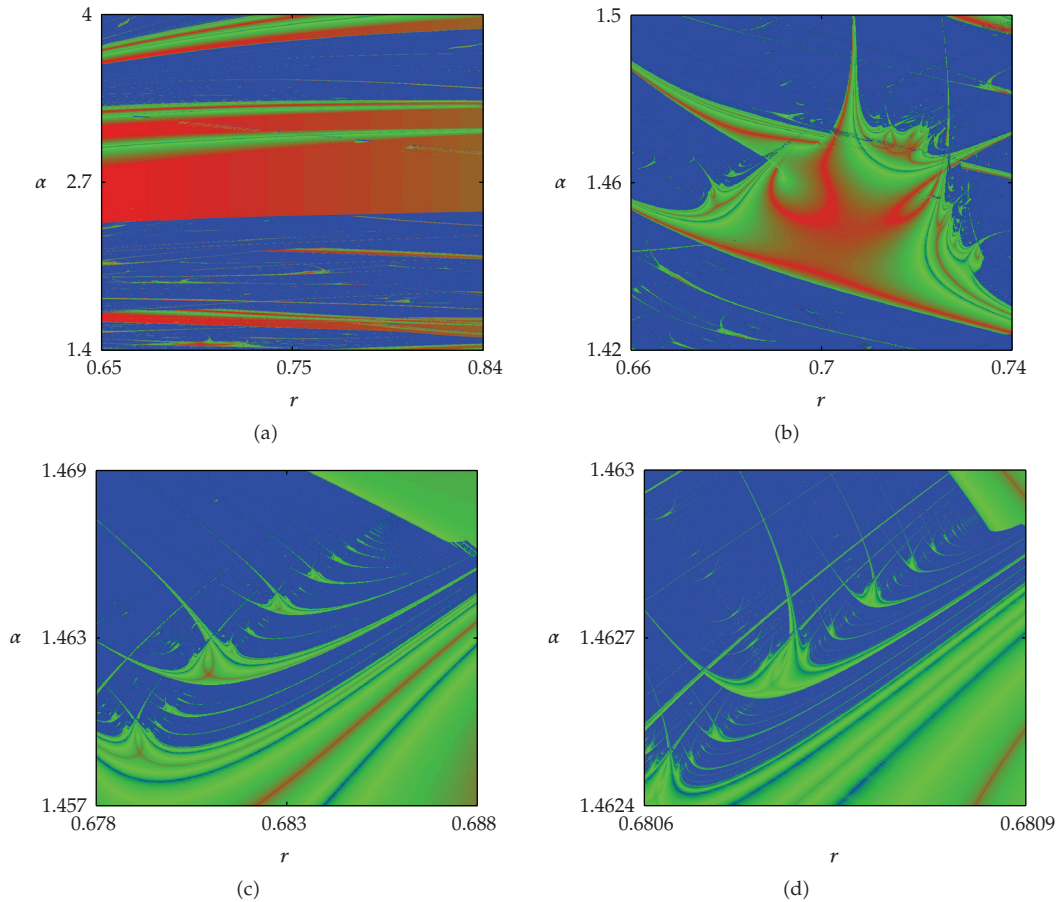


**Figure 6:** (a) Parameter space diagram with periodic structures. (b)–(d) Successive magnifications of parameter space diagram.

To finalize, in Figures 8(a) and 8(b) we depict two successive magnifications of the parameter space diagram (Figure 6(b)). In this case, we can observe a high concentration of periodic structures with different shapes (Figure 8(a)). These structures cross each other indicating coexistence of periodic attractors. In Figure 8(b), we identify a periodic structure that appears abundantly in parameter space, for the system considered, consisting of three shrimp shapes connected. In addition, we again observe crossings between periodic sets.

## 5. Conclusions

In this paper, we considered the impact-pair system studying its dynamics by a means of numerical simulations. Initially, we discussed the coexistence of attractors with smooth basin boundary, but with complicated and evolved basins structure. According to the uncertainty exponent evaluated for a certain region in phase space, this type basins of attraction is associated with effect of obstruction on predictability of time-asymptotic final state (attractor). In other words, the uncertainty in initial conditions leads to uncertainty in the final state.

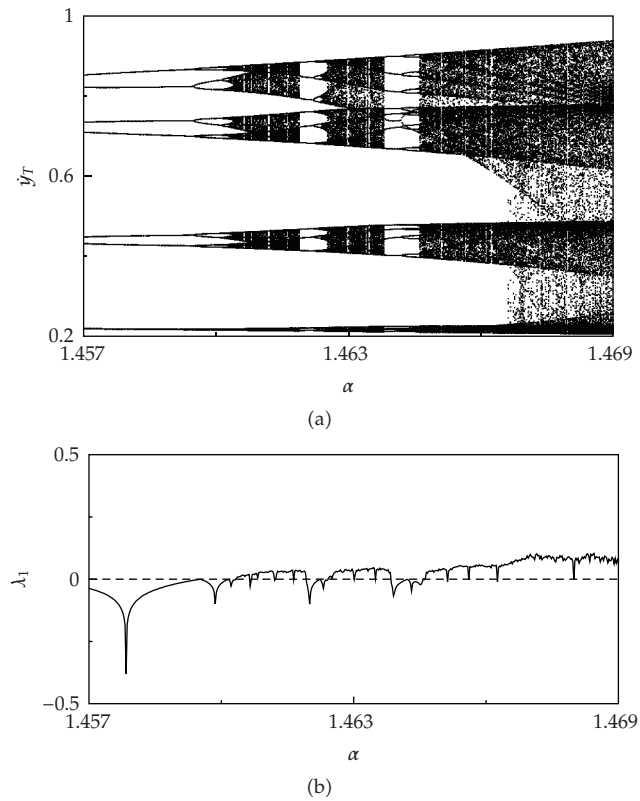


**Figure 7:** Bifurcation diagram of velocity  $\dot{y}_T$  as a function of the amplitude excitation  $\alpha$  for  $r = 0.683$ . (b) The largest Lyapunov exponents,  $\lambda_1$ , for attractors of the bifurcation diagram.

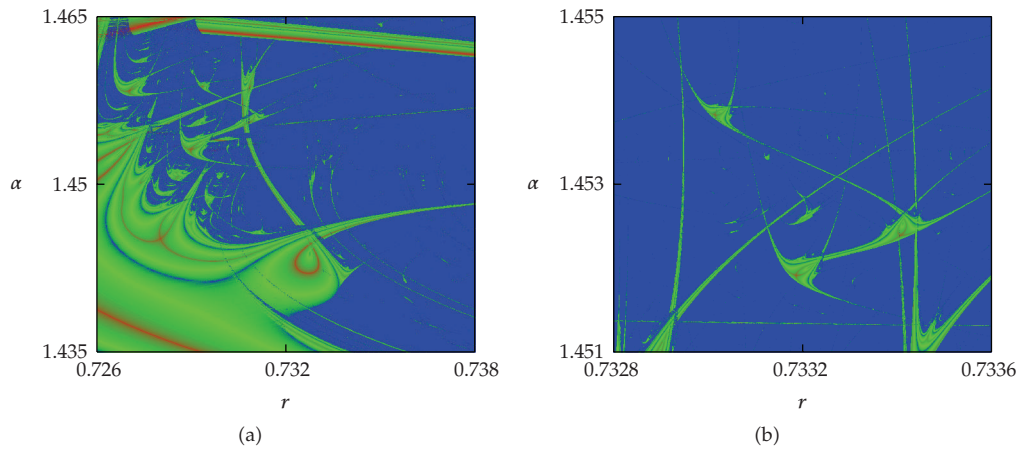


**Figure 8:** (a) Parameter space diagram with periodic structures. (b) Magnification of a portion of the previous figure.

In the end, we explored the dynamics in the two-dimensional parameter space by using the largest Lyapunov exponents. We identified several periodic sets embedded in chaotic region. Some of them, known as shrimps, present self-similar structures and organize themselves along a very specific direction in parameter space with a series of accumulations.

In addition, the periodic sets cross each other indicating a large quantity of coexisting periodic attractors.

## Acknowledgments

This work was made possible by partial financial support from the following Brazilian government agencies: FAPESP and CNPq.

## References

- [1] E. Fermi, "On the origin of the cosmic radiation," *Physical Review*, vol. 75, no. 8, pp. 1169–1174, 1949.
- [2] M. A. Lieberman and A. J. Lichtenberg, "Stochastic and adiabatic behavior of particles accelerated by periodic forces," *Physical Review A*, vol. 5, no. 4, pp. 1852–1866, 1972.
- [3] E. D. Leonel, P. V. E. McClintock, and J. K. L. Da Silva, "Fermi-Ulam accelerator model under scaling analysis," *Physical Review Letters*, vol. 93, no. 1, Article ID 014101, 4 pages, 2004.
- [4] E. D. Leonel and P. V. E. McClintock, "A hybrid Fermi-Ulam-bouncer model," *Journal of Physics A*, vol. 38, no. 4, pp. 823–839, 2005.
- [5] E. D. Leonel and P. V. E. McClintock, "A crisis in the dissipative Fermi accelerator model," *Journal of Physics A*, vol. 38, no. 23, pp. L425–L430, 2005.
- [6] D. G. Ladeira and E. D. Leonel, "Dynamical properties of a dissipative hybrid Fermi-Ulam-bouncer model," *Chaos*, vol. 17, no. 1, Article ID 013119, 7 pages, 2007.
- [7] F. Pfeiffer and A. Kunert, "Rattling models from deterministic to stochastic processes," *Nonlinear Dynamics*, vol. 1, no. 1, pp. 63–74, 1990.
- [8] S. L. T. de Souza, I. L. Caldas, R. L. Viana, and J. M. Balthazar, "Sudden changes in chaotic attractors and transient basins in a model for rattling in gearboxes," *Chaos, Solitons & Fractals*, vol. 21, no. 3, pp. 763–772, 2004.
- [9] S. L. T. de Souza, I. L. Caldas, R. L. Viana, A. M. Batista, and T. Kapitaniak, "Noise-induced basin hopping in a gearbox model," *Chaos, Solitons & Fractals*, vol. 26, no. 5, pp. 1523–1531, 2005.
- [10] S. L. T. de Souza, I. L. Caldas, R. L. Viana, and J. M. Balthazar, "Control and chaos for vibro-impact and non-ideal oscillators," *Journal of Theoretical and Applied Mechanics*, vol. 46, pp. 641–664, 2008.
- [11] S. Chatterjee, A. K. Mallik, and A. Ghosh, "On impact dampers for non-linear vibrating systems," *Journal of Sound and Vibration*, vol. 187, no. 3, pp. 403–420, 1995.
- [12] S. L. T. de Souza, I. L. Caldas, R. L. Viana, J. M. Balthazar, and R. M. L. R. F. Brasil, "Impact dampers for controlling chaos in systems with limited power supply," *Journal of Sound and Vibration*, vol. 279, no. 3–5, pp. 955–967, 2005.
- [13] M. Wiercigroch, A. M. Krivtsov, and J. Wojewoda, "Vibrational energy transfer via modulated impacts for percussive drilling," *Journal of Theoretical and Applied Mechanics*, vol. 46, pp. 715–726, 2008.
- [14] J. Jerrelind and H. Dankowicz, "A global control strategy for efficient control of a Braille impact hammer," *Journal of Vibration and Acoustics*, vol. 128, no. 2, pp. 184–189, 2006.
- [15] K.-C. Woo, A. A. Rodger, R. D. Neilson, and M. Wiercigroch, "Application of the harmonic balance method to ground moling machines operating in periodic regimes," *Chaos, Solitons & Fractals*, vol. 11, no. 13, pp. 2515–2525, 2000.
- [16] R. P. S. Han, A. C. J. Luo, and W. Deng, "Chaotic motion of a horizontal impact pair," *Journal of Sound and Vibration*, vol. 181, no. 2, pp. 231–250, 1995.
- [17] A. C. J. Luo, "Period-doubling induced chaotic motion in the LR model of a horizontal impact oscillator," *Chaos, Solitons & Fractals*, vol. 19, no. 4, pp. 823–839, 2004.
- [18] S. L. T. de Souza and I. L. Caldas, "Calculation of Lyapunov exponents in systems with impacts," *Chaos, Solitons & Fractals*, vol. 19, no. 3, pp. 569–579, 2004.
- [19] S. L. T. de Souza, A. M. Batista, I. L. Caldas, R. L. Viana, and T. Kapitaniak, "Noise-induced basin hopping in a vibro-impact system," *Chaos, Solitons & Fractals*, vol. 32, no. 2, pp. 758–767, 2007.
- [20] S. L. T. de Souza and I. L. Caldas, "Controlling chaotic orbits in mechanical systems with impacts," *Chaos, Solitons & Fractals*, vol. 19, no. 1, pp. 171–178, 2004.

- [21] J. A. C. Gallas, "Dissecting shrimps: results for some one-dimensional physical models," *Physica A*, vol. 202, no. 1-2, pp. 196–223, 1994.
- [22] L. Jin, Q.-S. Lu, and E. H. Twizell, "A method for calculating the spectrum of Lyapunov exponents by local maps in non-smooth impact-vibrating systems," *Journal of Sound and Vibration*, vol. 298, no. 4-5, pp. 1019–1033, 2006.
- [23] J. Aguirre, R. L. Viana, and M. A. F. Sanjuán, "Fractal structures in nonlinear dynamics," *Reviews of Modern Physics*, vol. 81, no. 1, pp. 333–386, 2009.
- [24] S. W. McDonald, C. Grebogi, E. Ott, and J. A. Yorke, "Fractal basin boundaries," *Physica D*, vol. 17, no. 2, pp. 125–153, 1985.
- [25] M. S. T. de Freitas, R. L. Viana, and C. Grebogi, "Multistability, basin boundary structure, and chaotic behavior in a suspension bridge model," *International Journal of Bifurcation and Chaos*, vol. 14, no. 3, pp. 927–950, 2004.
- [26] C. Grebogi, S. W. McDonald, E. Ott, and J. A. Yorke, "Final state sensitivity: an obstruction to predictability," *Physics Letters A*, vol. 99, no. 9, pp. 415–418, 1983.
- [27] J. Rössler, M. Kiwi, B. Hess, and M. Markus, "Modulated nonlinear processes and a novel mechanism to induce chaos," *Physical Review A*, vol. 39, no. 11, pp. 5954–5960, 1989.
- [28] O. De Feo, G. M. Maggio, and M. P. Kennedy, "The Colpitts oscillator: families of periodic solutions and their bifurcations," *International Journal of Bifurcation and Chaos*, vol. 10, no. 5, pp. 935–958, 2000.
- [29] O. De Feo and G. M. Maggio, "Bifurcations in the Colpitts oscillator: from theory to practice," *International Journal of Bifurcation and Chaos*, vol. 13, no. 10, pp. 2917–2934, 2003.
- [30] M. Kawamura, R. Tokunaga, and M. Okada, "Bifurcation analysis in an associative memory model," *Physical Review E*, vol. 70, no. 4, Article ID 046210, 9 pages, 2004.
- [31] V. Castro, M. Monti, W. B. Pardo, J. A. Walkenstein, and E. Rosa Jr., "Characterization of the Rössler system in parameter space," *International Journal of Bifurcation and Chaos*, vol. 17, no. 3, pp. 965–973, 2007.
- [32] C. Bonatto, J. C. Garreau, and J. A. C. Gallas, "Self-similarities in the frequency-amplitude space of a loss-modulated CO<sub>2</sub> laser," *Physical Review Letters*, vol. 95, no. 14, Article ID 143905, 4 pages, 2005.
- [33] C. Bonatto and J. A. C. Gallas, "Periodicity hub and nested spirals in the phase diagram of a simple resistive circuit," *Physical Review Letters*, vol. 101, no. 5, Article ID 054101, 2008.
- [34] H. A. Albuquerque, R. M. Rubinger, and P. C. Rech, "Self-similar structures in a 2D parameter-space of an inductorless Chua's circuit," *Physics Letters A*, vol. 372, no. 27-28, pp. 4793–4798, 2008.